ACS APPLIED MATERIALS & INTERFACES

www.acsami.org

Research Article

High-Pressure Synthesis and Gas-Sensing Tests of 1-D Polymer/Aluminophosphate Nanocomposites

Frederico G. Alabarse,* Michelangelo Polisi, Marco Fabbiani, Simona Quartieri, Rossella Arletti, Boby Joseph, Francesco Capitani, Sylvie Contreras, Leszek Konczewicz, Jerome Rouquette, Bruno Alonso, Francesco Di Renzo, Giulia Zambotti, Marco Baù, Marco Ferrari, Vittorio Ferrari, Andrea Ponzoni,* Mario Santoro,* and Julien Haines*

Cite This: *ACS Appl. Mater. Interfaces* 2021, 13, 27237−27244

Read Online

ACCESS | Metrics & More | Article Recommendations | Supporting Information

ABSTRACT: Recently, filling zeolites with gaseous hydrocarbons at high pressures in diamond anvil cells has been carried out to synthesize novel polymer-guest/zeolite-host nanocomposites with potential, intriguing applications, although the small amount of materials, 10^{-7} cm^3, severely limited true technological exploitation. Here, liquid phenylacetylene, a much more practical reactant, was polymerized in the 12 Å channels of the aluminophosphate Virginia Polytechnic Institute—Five (VFI) at about 0.8 GPa and 140 °C, with large volumes in the order of 0.6 cm^3. The resulting polymer/VFI composite was investigated by synchrotron X-ray diffraction and optical and ^{1}H, ^{13}C, and ^{27}Al nuclear magnetic resonance spectroscopy. The materials, consisting of disordered π-conjugated polyphenylacetylene chains in the pores of VFI, were deposited on quartz crystal microbalances and tested as gas sensors. We obtained promising sensing performances to water and butanol vapors, attributed to the finely tuned nanostructure of the composites. High-pressure synthesis is used here to obtain an otherwise unattainable true technological material.

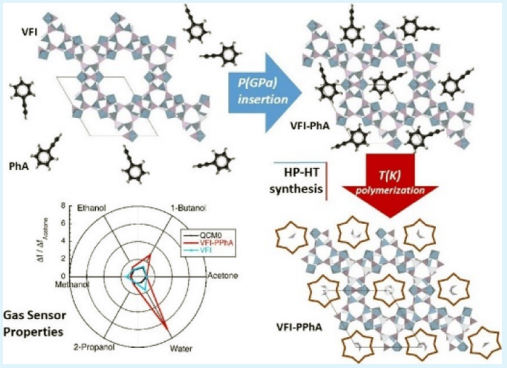

KEYWORDS: *nanocomposites, high-pressure synthesis, gas sensing, polymer, aluminophosphate*

INTRODUCTION

Since its advent more than one century ago, high pressure (P > 0.1 GPa) science and technology offered a versatile approach to synthesize materials with unusual properties. For example, by exploring ranges in the temperature−pressure space that are outside the domain of conventional synthesis techniques, the metallic phase of sulfur hydrides exhibiting superconductivity up to 203 K was synthesized.[1] Nonetheless, owing to difficulties in recovering materials at room pressure and the low production rate, the technological exploitation of high-pressure materials is still limited to very few examples such as low-density polyethylene,[2] diamond,[3] cubic boron nitride,[4] and maybe, potentially, carbon nanothreads.[5] Here, we synthesized a unique 1D polyphenylacetylene (PPhA)/aluminophosphate nanocomposite with promising gas-sensing properties and potential for large-scale production, where high pressure is the unavoidable key enabling synthesis methodology.

PPhA is a π-conjugated system, which has potential applications in organic electronics as a conductive polymer. Polymerization of phenylacetylene (PhA) can be induced by catalysts, temperature, and pressure (see ref 6 and references therein) with some differences in the structure of the obtained polymer in terms of the isomers and conformers present. Polymerization under pressure in confined molecular systems such as those inserted in zeolites can be used to select a particular isomer with its unique associated physical properties. In the case of acetylene polymerized in purely siliceous zeolites at pressures of about 5 GPa, trans and cis isomers are obtained selectively, depending on the zeolite pore topology.[7,8] Density functional theory calculations indicate that the trans isomer is metallic, whereas the cis form is a narrow band gap semiconductor.[8] Preparing similar isolated, densely packed polymeric chains featuring molecular-sized diameter is very challenging due to the tendency of these chains to bend and aggregate into fibers, hence losing the molecular size and the related properties.[9] Hence, the idea of confining single polymer chains into the channels of host zeolites arose. These novel hybrid polymer/host-zeolite materials should feature, in principle, a unique combination of remarkable physical

Received: January 11, 2021
Accepted: April 16, 2021
Published: June 3, 2021

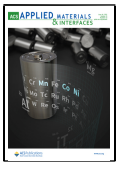

https://doi.org/10.1021/acsami.1c00625
ACS Appl. Mater. Interfaces 2021, 13, 27237−27244

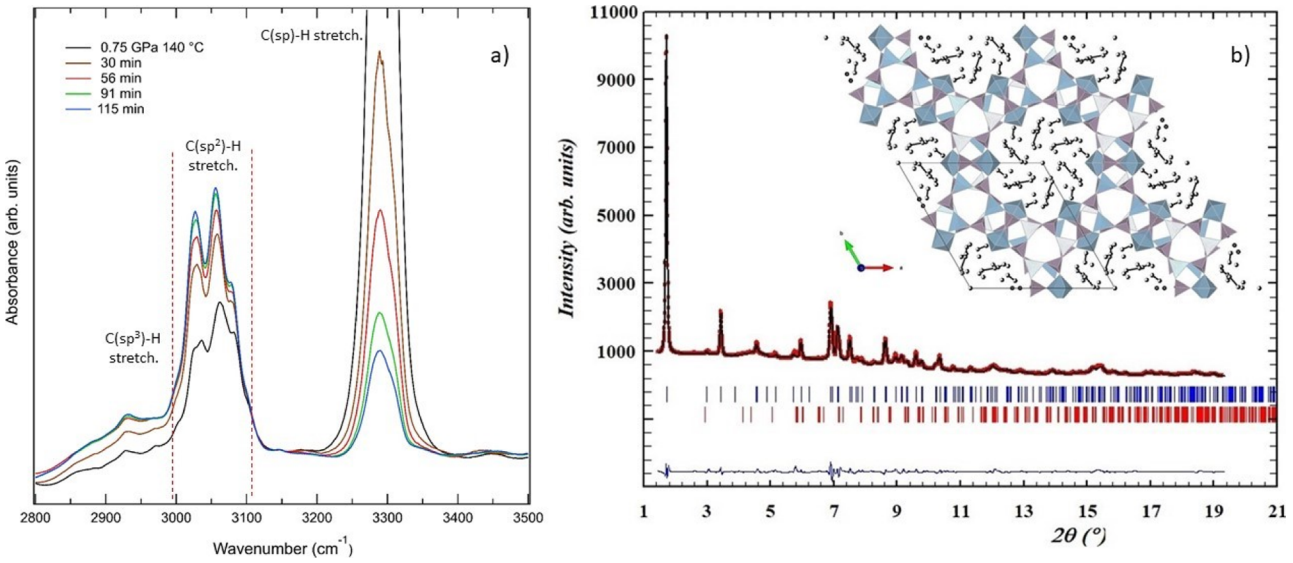

Figure 1. (a) Tracking *in situ* and in real time the polymerization process. Time evolution of *in situ* IR absorption spectra (30 μm beam spot) measured on a VFI single crystal, which was loaded in a DAC and compressed in PhA at 0.75 GPa at 140 °C. Thin layers of pure PhA on the top and bottom of the crystal contribute negligibly to the IR absorption signal. (b) Crystal structure of the VFI−PPhA composite. The observed and calculated powder XRD pattern collected *ex situ* from the large-volume VFI−PPhA nanocomposite sample (blue tick marks) recovered after compression of preloaded VFI in liquid PhA at 0.6 GPa and 130 °C for 45 min (λ = 0.4957 Å). Trace quantities of a hydrated impurity ($AlPO_4$-H_3, red tick marks) were present as a secondary phase. Final agreement factors were R_p = 13.5%, R_{wp} = 11.9%, and *R*-bragg = 4.0%. Inset: unit cell (outlined in black) and structure obtained by Rietveld refinement. The light-blue and purple polyhedra are the AlO_4, AlO_6, and PO_4 units of VFI, while the black circles in the pore indicate C atoms from the inserted polymer and any O atoms from H_2O molecules.

properties, such as a huge surface area of the host material joint with quantum confinement of the π-conjugated polymer. Examples and discussion on quantum confinement on similar systems can be found elsewhere.[8] These properties could be expected to be strongly enhanced with respect to those of polymers confined in other systems with larger pores such as metal−organic frameworks[10,11] or mesoporous materials.[12,13] Such physical properties have strong potential for several technological applications, such as those in the gas-sensing field. Indeed, in this field, micro-/mesoconfinement of the polymer appears to be an advantage. As a matter of fact, size effects were widely reported in the literature, with improved gas-sensing performance correlating well with decreasing diameter of the polymer fibers[14,15] and X-ray photoelectron spectrometry showing that gaseous molecules penetrate in PPhA up to a depth of about 2 nm.[16,17]

In the present study, we target the polymerization at moderate high pressures and temperatures (*i.e.*, compatible with large-scale industrial production) of liquid PhA in the channels of the aluminophosphate Virginia Polytechnic Institute—Five (VFI), characterized by a hexagonal structure with a 1D pore system with diameters of 12.7 Å, which are the largest pores known for zeolites and aluminophosphates. $AlPO_4$-54·xH_2O (hexagonal VFI structure) exhibits 1-D hydrophilic pores along the c direction, in which H_2O molecules form a disordered hydrogen-bonded network.[18,19] The pore water can be easily removed by exposing the material to vacuum,[20,21] leaving the 1-D nanochannels free for insertion of guest molecules. The aluminophosphate framework is built up of 4-, 6-, and 18-membered rings of alternating AlO_6, AlO_4, and PO_4 polyhedra, which constitute a host matrix. One-third of the aluminum cations are octahedrally coordinated due to the presence of two H_2O molecules in their coordination sphere. In fact, VFI can, in principle, accommodate PPhA in its large nanopores, while this polymer is not expected to fit the smaller pores of purely siliceous zeolites. The novel nanocomposite materials were characterized by synchrotron X-ray diffraction (XRD) and Raman, infrared (IR), and nuclear magnetic resonance (NMR) spectroscopy. We further deposited the prepared materials on quartz crystal microbalances (QCMs) to test their performance in gas sensors.

RESULTS AND DISCUSSION

Material Synthesis Methodologies. The materials were first studied *in situ* at high pressure and high temperature in diamond anvil cells (DACs) using distinct synthesis protocols ($P-T$ paths), which led to very small volumes of the product in the range of 10^{-7} cm^3. After that, guided by the *in situ* material characterization, large-volume samples ($\leq$1 cm^{-3}) were prepared under optimized $P-T$ conditions in a gas bomb for the *ex situ* analysis to be performed on the samples recovered under ambient conditions. In fact, while DACs provide access to X-ray, IR, and visible radiation through the diamonds, the large-volume cell (see "Large-volume synthesis" in the Supporting Information) does not permit access for these radiation probes. In both types of cells, partially dehydrated VFI powder or single crystals were loaded in the synthesis chamber together with purified and dried liquid PhA. In one case, VFI was preloaded with purified dry PhA by direct adsorption in the gas phase prior to loading it in the large-volume cell together with additional liquid PhA. Bulk PPhA samples were also prepared using purified−dehydrated dry PhA for comparison. The large-volume nanocomposite materials were obtained by pressurizing the initial VFI−PhA mixtures to 0.6−0.8 GPa and heating them to 114−140 °C for about 1−2 h, corresponding to the optimal $P-T$-time synthesis conditions. A more detailed description of the synthesis methodologies is reported in the "Materials and methods" section from the Supporting Information, where we also show how the synthesis protocol was optimized as a function of high

https://doi.org/10.1021/acsami.1c00625
ACS Appl. Mater. Interfaces 2021, 13, 27237−27244

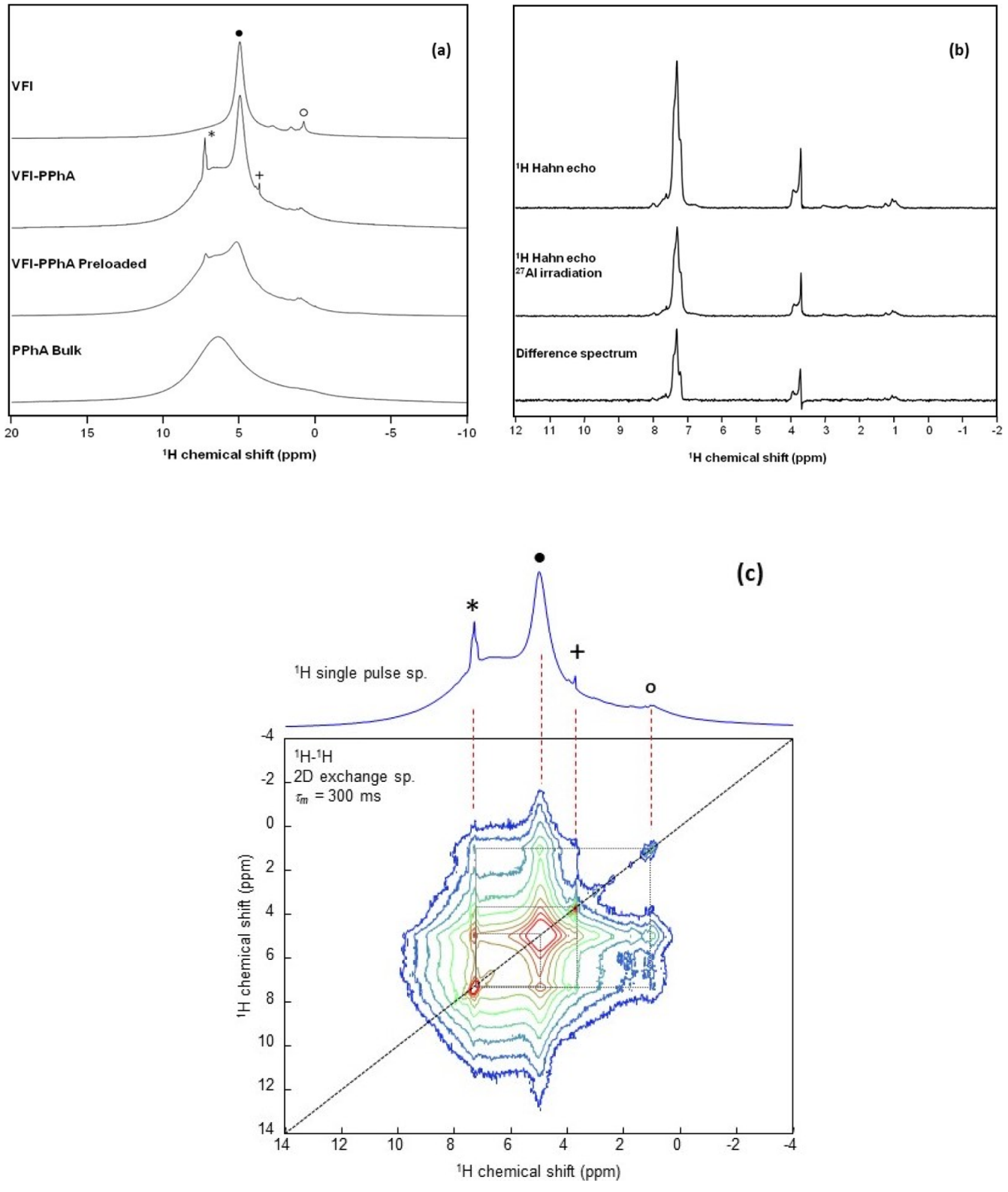

Figure 2. *Ex situ* NMR spectroscopy analysis of the polymerization process occurring in the large-volume VFI−PPhA sample. ^{1}H NMR single-pulse MAS spectra (ν_{MAS} = 17−18 kHz) of hydrated VFI, VFI−PPhA, preloaded VFI−PPhA, and bulk PPhA samples (a), where the symbols are assigned by (*) ^{1}H from the aromatic rings and (+) ^{1}H from cyclohexadienyl defect groups from the PPhA polymer, (•) ^{1}H from the physically adsorbed H_2O in the pores, and (O) the ^{1}H from structural H_2O linked to ^{VI}Al. ^{1}H {^{27}Al} TRAPDOR NMR experiments on VFI−PPhA (b). The ^{1}H spectrum at the top corresponds to a Hahn echo with delays τ = 8.8 ms synchronized with MAS (ν_{MAS} = 18 kHz). The ^{1}H spectrum in the middle is obtained with additional ^{27}Al irradiation during the first echo delay. The difference between both spectra is presented at the bottom. ^{1}H−^{1}H 2D exchange NMR spectrum of the VFI−PPhA sample (c) obtained for a long mixing time τ_m = 300 ms (ν_{MAS} = 18 kHz).

https://doi.org/10.1021/acsami.1c00625
ACS Appl. Mater. Interfaces 2021, 13, 27237−27244

pressures and temperatures, which are mandatory for obtaining the maximum filling of VFI by PhA and for activating the polymerization of PhA without affecting the stability of the VFI host structure.

***In Situ* XRD and IR Studies of Material Synthesis.** Crystalline VFI was observed to be stable in the pressure (P) domain investigated at room temperature (T) based on XRD data of VFI compressed in PhA in the DAC, Figure S4 (section "*In situ* high-pressure measurements using diamond anvil cells" in the Supporting Information). The measured unit cell parameters and volume are clearly higher than those of empty VFI, indicating the pressure-induced pore filling[21] and, consequently, that high pressure is a mandatory tool for the purpose of synthesizing PPhA in the VFI micropores.

IR spectroscopy was used to identify the chemical nature of the PPhA polymer synthesized in the VFI channels. IR spectra of a VFI single crystal compressed in PhA in a DAC at 0.75 GPa and 140 °C enabled the *in situ* polymerization of the inserted monomer to be followed as a function of time, Figure 1a. Indeed, the ≡C−H stretching band at 3300 cm^{-1} for monomeric sp carbon is drastically reduced in intensity during the thermal treatment. This is accompanied by an intensity increase at 3100−3000 cm^{-1} where C−H stretching vibrations from sp^2 carbon are typically found, signaling the formation of the 1D-conjugated ···−C═C−C═C−C═C−C═C−··· backbone of PPhA, which is a 1D polyacetylene-like chain where half of the hydrogen atoms are substituted by phenyl groups. The C−H stretching signature of this skeleton partially overlaps with that of the aromatic phenyl groups of both molecular and polymeric PhA (also at 3100−3000 cm^{-1}), which are substantially unaltered during the polymerization process. In particular, a sharp peak at around 3027 cm^{-1} increases, which again is the sign of a 1D-conjugated system of sp^2 carbon. An intensity increase at 3000−2800 cm^{-1} is also observed, due to C−H stretching modes of saturated sp^3 C defects.

Large-Volume Synthesis and *Ex Situ* Material Characterization by XRD and IR, Raman, and NMR Spectroscopy. The XRD pattern of an orange-yellow, large-volume sample (VFI preloaded with PhA) after treatment at 0.6 GPa and 130 °C, whose color indicated that a π-conjugated polymer was indeed formed from PhA, was measured on the Xpress beamline (Elettra). Rietveld refinements were performed using a starting model for the Al−O−P framework taken from previous studies.[18,19] Fourier difference synthesis was used to locate guest atoms in the pores. Only the occupation factors of the guest atoms were refined. Agreement factors were strongly improved by considering a filled model compared to the empty one. Partial rehydration had occurred, giving rise to fully occupied sites in the octahedra with structural H_2O. As in hydrated VFI, significant disorder is observed for the guest species in the pores, which does not allow the exact positions of the PPhA chains to be located (Figure 1b, Table S2 in the Supporting Information). It is also probable that there are some adsorbed H_2O molecules between the PPhA chains and the pore walls.

The large-volume VFI−PPhA nanocomposites were also studied *ex situ* by IR and Raman spectroscopy (full details in the section "*Ex situ* characterization of VFI−PPhA nanocomposites by XRD and IR, Raman, and NMR spectroscopy" in the Supporting Information), as *in situ* high P−T synthesis in DACs (see above), the polymerization of confined PhA is almost complete after treatments at 0.6−0.8 GPa and 125−130 °C and the embedded polymer indeed consists of π-conjugated PPhA chains with some sp^3 C defects. Importantly, in all recovered samples, partial rehydration was observed, corresponding to some amount of water entering in between the polymeric chains confined in VFI and the strongly hydrophilic zeolite framework. This is a fundamental result in view of the exploitation of these materials as gas sensors. It confirms that gas molecules can access the inner volume of the VFI, where they may interact with the target PPhA nanochains.

The large-volume VFI−PPhA nanocomposite samples were investigated by $^{13}C\{^1H\}$ (see the section "*Ex situ* characterization of VFI−PPhA nanocomposites by XRD and IR, Raman, and NMR spectroscopy" in the Supporting Information) and ^1H solid-state NMR. Single-pulse ^1H MAS NMR spectra are presented in Figure 2a. Complex spectra were obtained with both sharp and broad peaks. Additional measurements were performed on bulk PPhA and on hydrated VFI. It can be seen that the two broad peaks found for the bulk polymer are also present in the VFI−PPhA samples along with the peaks of physically adsorbed ($\delta_{iso} \approx 5$ ppm) and octahedral structural H_2O (δ_{iso} = 0.7−1.0 ppm) from the VFI host.[22−24] The physically adsorbed H_2O peak was slightly weaker in the VFI−PPhA sample than in hydrated VFI and much weaker in the VFI−PPhA sample preloaded with the PhA vapor before the high P−T synthesis, which can be linked to the partial dehydration and rehydration process. Additional sharp peaks are present in the spectra of the VFI−PPhA samples at δ_{iso} = 7.3−7.5 ppm and δ_{iso} = 3.6−4.0 ppm. These resonances can be assigned to the protons of aromatic rings (*) and cyclohexadienyl groups (+), respectively. The resonances at δ_{iso} = 3.6−4.0 ppm have been observed previously in certain PPhA samples[25] and correspond to terminal groups or defects in the PPhA chains. The narrow linewidth of these peaks could be an indication of a higher degree of mobility for these groups. These peaks are significantly weaker in the preloaded sample, indicating that the polymerization has occurred to a greater extent (*i.e.*, longer chains with less mobile aromatic groups) and fewer defects are present. It will be shown below that a contribution to the broad peaks arises from the polymer in the pores of VFI. There is no evidence of the presence of the remaining PhA monomer ($\delta_{iso} \approx 3$ ppm). This indicates that full polymerization had occurred, in agreement with the IR and Raman spectroscopy results.

Additional experiments were performed to probe the organic species located inside the VFI pores in the non-preloaded VFI−PPhA sample. $^1H\{^{27}Al\}$ TRAPDOR NMR experiments[26] based on ^1H−^{27}Al dipolar coupling were performed to investigate H−Al distances (<10 Å). The use of long delays between ^1H echo pulses insures an efficient dephasing effect for the ^{27}Al irradiation but acts as a T_2 filter removing the broad resonances with short ^1H transverse relaxation times. Nevertheless, the sharp peaks from the aromatic rings and the cyclohexadienyl groups from the PPhA polymer and the structural H_2O were observed in the difference spectrum, Figure 2b. This is evidence that these protons are located in the pores of VFI. ^1H−^1H 2D exchange spectra allowing for proton spin diffusion to proceed were also acquired to determine which signals arise from the same phase in the 1−100 nm scale range[27] in the VFI−PPhA sample. For a long mixing time, off-diagonal correlations are observed between the resonances of aromatic (*) and cyclohexadienyl (+) protons from the PPhA polymer and the adsorbed (•) and structural (^{O}) H_2O protons from VFI (Figure 2c). It should be

https://doi.org/10.1021/acsami.1c00625
ACS Appl. Mater. Interfaces 2021, 13, 27237−27244

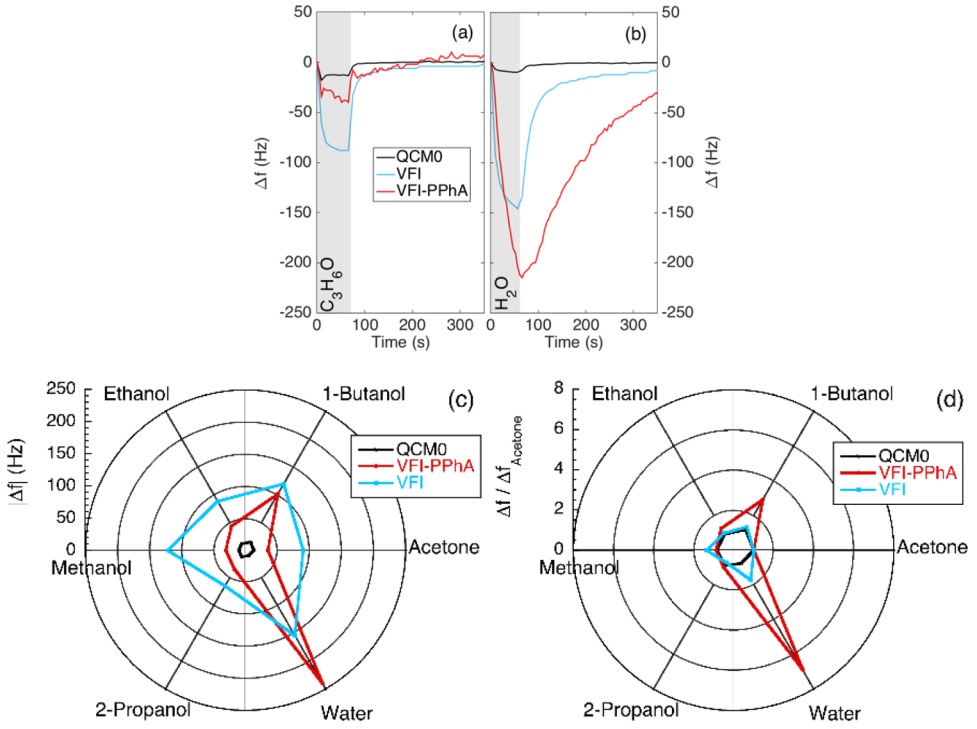

Figure 3. Functional characterization of the prepared gas sensors. Time dependence of sensor responses (frequency shift, Δf) to vapors of acetone, C_3H_6O, (a) and water, H_2O, (b). Both compounds were tested at a concentration of 12% of their saturated vapor pressure. Polar plots of the responses measured with sensors based on pristine QCM (QCM0), QCM functionalized with VFI powders (VFI), and QCM functionalized with VFI−PPhA powders (VFI−PPhA) exposed to different vapors, each one tested at a concentration of 12% of its respective vapor pressure: sensor response expressed as the absolute frequency shift, $|\Delta f|$, (c) and as frequency shift normalized to the shift measured with acetone (d).

noted that the off-diagonal correlation with structural H_2O protons from VFI also concerns the broad resonance of aromatic carbons in the PPhA polymer located at $\delta_{iso} \approx 6.5$ ppm. This is consistent with the polymerization taking place inside the pores of VFI.

The combined NMR data are consistent with the polymerization of PhA around and within the microstructure of polycrystalline VFI, which consists of aggregated polycrystals in a butterfly form made of $30 \times 1 \times 1$ μm^3 crystals with some empty space between them. The inserted polymer corresponds to PPhA with different amounts of cyclohexadienyl defects depending on the degree of pore filling. A high degree of pore filling obtained by preloading VFI in the vapor phase reduces both the amount of defects in the confined polymer and the water content due to rehydration.

Gas-Sensing Measurements. Gas-sensing tests were carried out to investigate the potentialities of the VFI−PPhA composite and to look for the contribution of the confined PPhA chains. The behavior of the composite material is quite complex; indeed, we may expect functionalities arising from both VFI and PPhA. Diffusion and polarity effects are typically invoked to explain the behavior of zeolite-based sensors,[28] while polymers are usually reported to interact with the gases *via* chemical reactions involving charge transfer or *via* weak intermolecular forces such as H-bonding and $\pi-\pi$ and dipole−dipole interactions.[15] QCM sensors have been functionalized by the drop-casting method according to the procedure described in the Supporting Information.

As an example, Figure 3a,b reports the sensor signal measured with our three test samples, namely, the pristine QCM sensor (QCM0) and the QCM sensor functionalized with either the VFI powders (VFI) or the VFI−PPhA powders (VFI−PPhA), against water and acetone vapors, both tested at a partial pressure of 12% of their own saturated vapor pressure ($0.12p_0$).

A more complete overview of the sensing properties of these materials can be observed in Figure 3c, which reports the response pattern of the three sensors against the six vapors, each measured at a $0.12p_0$ partial pressure. Three observations can be made from this plot: (i) the response intensity of the pristine QCM (QCM0) is much weaker than the response of the functionalized devices, whichever the gas used. This can be reasonably ascribed to the structural and morphological features of both VFI and VFI−PPhA materials, namely, their large surface area and the size of the isolated polymeric chains. Indeed, although in our composite material, PPhA is present both as isolated chains and as bulk structures, IR and NMR spectroscopic investigations suggest that water molecules have room to access the inner pores and that most of the PPhA is inside the host cavities, hence in the nanostructured form. Moreover, this latter form will benefit from the large surface area of the porous inner volume of the host VFI crystals, in contrast to the bulk phase, which will interact with gases only through the much lower surface area given by the external area of the grains. Based on the combination of these findings, we may reasonably suggest that the PPhA contribution will mainly arise from the target nanostructures rather than from the bulk. (ii) Among the tested vapors, water induces the largest response both in VFI and VFI−PPhA sensors. This may be partially explained by considering the synergic action of the hydrophilic properties of VFI with the PPhA affinity to this molecule,[16,25,29,30] but the aforementioned structural and morphological features of our composite material are also likely to play a role. Compared with the PPhA literature, in

https://doi.org/10.1021/acsami.1c00625
ACS Appl. Mater. Interfaces 2021, 13, 27237−27244

which a response of about 130 Hz to water vapors ($0.15p_0$)[30] was achieved after morphological and compositional optimization of the PPhA layer, the 239 ± 23 Hz shift recorded in the present work with the VFI−PPhA sensors ($0.12p_0$) is at least competitive. (iii) VFI and VFI−PPhA feature different response patterns, indicating the active role of PPhA in the composite material. From the application viewpoint, this is a fundamental characteristic. Indeed, since gas sensors are not chemically selective, selectivity is achieved by integrating these devices in more complex systems. The so-called electronic nose is one of the most popular among these systems. It is based on an array of different partially selective gas sensors, combined with a pattern recognition software that correlates the array response to the smelled atmospheres.[31] The need for sensors featuring different response patterns to chemicals is probably among the largest stimuli for sensing oriented materials science research.

To better visualize the partial specificity, it is worth normalizing the response pattern to the response of a reference compound, for example, acetone (Figure 3d). Expressing the vapor amount as fractions of the respective vapor pressure p_0 helps to gain further insights into the role played by the nanostructured PPhA in the VFI−PPhA composite, in particular, about the nonspecific partition of vapors into polymers, which is often reported in the gas-sensing literature when working with homologous analytes, such as alcohols.[32] In our case, the marked partial specificity to butanol finds neither correspondence in the VFI sensor (Figure 3) nor in the PPhA literature (see "Gas-sensing characterization" in the Supporting Information), in which, however, our extreme lateral confinement was never achieved. Hence, we find it reasonable to ascribe this feature to the molecular-scale cross section of the prepared PPhA chains.

CONCLUSIONS

We synthesized a novel π-conjugated polymer/porous aluminophosphate nanocomposite of the guest PPhA/host VFI type under moderately high $P-T$ conditions of 0.8 GPa and 140 °C. This $P-T$ combination resulted to be the optimum condition for three simultaneous mandatory requirements: (i) the maximum filling of VFI by the reacting PhA monomer and, consequently, by the product PPhA polymer by taking into account steric constraints, (ii) the almost complete polymerization of the monomer, and (iii) the stability of the host VFI framework for the inserted polymer with respect to other microporous (such as $AlPO_4$-8) and nonporous (such as berlinite or tridymite) $AlPO_4$ phases. VFI−PPhA nanocomposites are composed of PPhA confined in the VFI scaffold. Our results demonstrate a new strategy/protocol to synthesize isolated, single-chain nanostructured π-conjugated polymers, nanoconfined in an insulating matrix. Such a novel material and its synthesis protocol may be transferred to industrial large-scale production through large-volume (cm^3) HP cells. Preliminary gas-sensing tests showed the potentialities of the prepared VFI−PPhA material in terms of sensitivity and partial selectivity to water and butanol vapors, which can be reasonably ascribed to the large surface area of the composite and the extreme reduction of the PPhA chain cross section.

METHODS

Material Synthesis in DACs. VFI powder or single crystals were loaded in DACs along with a ruby pressure gauge in the hole of the metal gasket, having a diameter and thickness of 150−250 and 30−50 μm, respectively. The open DAC together with the sample was exposed to vacuum before being transferred to a glovebox under a controlled Ar or N_2 atmosphere. Purified and dried liquid PhA was then added to the sample before the DAC was hermetically closed inside the glovebox. A detailed description about the host material and guest molecule preparation is found in the Supporting Information (sections "Host material: dehydrated VFI" and "*In situ* high pressure measurements using diamond anvil cells" in the Supporting Information). This procedure was employed for the samples studied by *in situ* XRD and IR spectroscopy.

Material Synthesis in Large-Volume Cells. As for the DAC experiments, the VFI powder or single crystals, used for the larger-volume experiments, were partially dehydrated in a glovebox entrance chamber and placed inside a PTFE capsule with an internal volume of 0.58 cm^3 and purified dry PhA was added under an Ar atmosphere in the glovebox. See a more detailed description in the Supporting Information (section "Large-volume synthesis: VFI−PPhA nanocomposite"). An additional sample was prepared from partially dehydrated VFI, which had been preloaded with purified dry PhA by direct adsorption in the gas phase and which was then introduced in the glovebox in a sealed glass tube under argon and transferred to the PTFE capsule with the addition of excess liquid PhA. The capsule was placed in a high-pressure chamber equipped with a resistive heater, which was pressurized to 0.6−0.8 GPa and heated to 114−140 °C for about 1−2 h.

Optimization of the Synthesis Protocol. Experiments were performed both *in situ* (at high P) and *ex situ* (samples recovered from the DAC or large-volume device at ambient P) using synchrotron XRD and IR on more than 20 distinct samples in order to establish the best protocol for loading PhA in dehydrated VFI in the high-pressure (HP) cells and to achieve full high $P-T$ polymerization of PhA in VFI without perturbing the phase of the host material. The selected samples corresponding to these optimal conditions are described in detail in this paper, in contrast to samples in which, for example, no polymerization occurred at an insufficiently high temperature (T < 110 °C) or for which transformation of VFI occurred at either too high pressure (P > 1 GPa) or high temperature (T > 150 °C). In addition, proper dehydration conditions of the starting VFI phase such as the vacuum pressure range and the time needed as described above are essential requirements (see ref 21) for obtaining a VFI−PPhA nanocomposite with as much as ideal structural and chemical properties. Applying pressure of a few tenths of GPa to the PhA−VFI mixture was a necessary requirement to achieve a complete filling of VFI by the monomer, while, at above 1 GPa, VFI undergoes a partial phase transition to the distinct porous-phase $AlPO_4$-8.[20]

Since liquid monomeric PhA is chemically stable below 1 GPa at room temperature, we heated the samples up to 130−140 °C, at around 0.6−0.8 GPa, in order to activate the polymerization of PhA in the initial PhA−VFI mixture within the timescale of a few hours or less and thus found the optimal conditions for the synthesis of the nanocomposite. On the other hand, at higher temperatures, VFI underwent phase transition to stable nonporous berlinite and tridymite forms of $AlPO_4$.

Material Characterization Methods. Methods for XRD, Raman, and IR spectroscopy, NMR, and gas-sensing tests are described in the Supporting Information.

Gas-Sensing Characterization Methods. The setup and measurement protocols adopted for gas-sensing tests are described in the Supporting Information.

ASSOCIATED CONTENT

Supporting Information

The Supporting Information is available free of charge at https://pubs.acs.org/doi/10.1021/acsami.1c00625.

Host material: dehydrated VFI; *in situ* high-pressure measurements using DACs; large-volume synthesis: VFI−PPhA nanocomposite; optimization of the syn-

https://doi.org/10.1021/acsami.1c00625
ACS Appl. Mater. Interfaces 2021, 13, 27237−27244

thesis protocol; *ex situ* analysis of VFI-PPhA nanocomposites; functionalization of QCM devices; *in situ* XRD investigations of the synthesis of VFI−PPhA nanocomposites; *ex situ* characterization of VFI-PPhA nanocomposites by XRD and IR, Raman, and NMR spectroscopy; and gas-sensing characterization (PDF)

AUTHOR INFORMATION

Corresponding Authors

Frederico G. Alabarse − *Elettra Sincrotrone Trieste, Trieste 34149, Italy;* orcid.org/0000-0002-7375-3666; Phone: +39.337.127.0679; Email: frederico.alabarse@elettra.eu; Fax: +39.040.938.0904

Andrea Ponzoni − *Istituto Nazionale di Ottica, INO-CNR, and Dipartimento di Ingegneria dell'Informazione, Università degli Studi di Brescia, Brescia 25121, Italy;* Phone: +39.030.3711.440; Email: andrea.ponzoni@ino.cnr.it; Fax: +39.030.6525.247

Mario Santoro − *Istituto Nazionale di Ottica, INO-CNR, and European Laboratory for Non Linear Spectroscopy, LENS, Sesto Fiorentino 50019, Italy;* orcid.org/0000-0001-5693-4636; Phone: +39.055.457.2490; Email: santoro@lens.unifi.it

Julien Haines − *ICGM, CNRS, Université de Montpellier, ENSCM, Montpellier 34095, France;* Phone: +33.4.67.14.93.49; Email: julien.haines@umontpellier.fr; Fax: +33.4.67.14.42.90

Authors

Michelangelo Polisi − *Dipartimento di Scienze Chimiche e Geologiche, Università di Modena, Modena 41121, Italy*

Marco Fabbiani − *Dipartimento di chimica, Università di Torino, Torino 10125, Italy;* orcid.org/0000-0002-9094-0279

Simona Quartieri − *Dipartimento di Scienze Chimiche e Geologiche, Università di Modena, Modena 41121, Italy*

Rossella Arletti − *Dipartimento di Scienze della Terra, Università di Torino, Torino 10125, taly*

Boby Joseph − *Elettra Sincrotrone Trieste, Trieste 34149, Italy;* orcid.org/0000-0002-3334-7540

Francesco Capitani − *Synchrotron Soleil, Gif sur Yvette 91192, France;* orcid.org/0000-0003-1161-7455

Sylvie Contreras − *Laboratoire Charles Coulomb, CNRS, Université de Montpellier, Montpellier 34095, France*

Leszek Konczewicz − *Laboratoire Charles Coulomb, CNRS, Université de Montpellier, Montpellier 34095, France*

Jerome Rouquette − *ICGM, CNRS, Université de Montpellier, ENSCM, Montpellier 34095, France*

Bruno Alonso − *ICGM, CNRS, Université de Montpellier, ENSCM, Montpellier 34095, France;* orcid.org/0000-0002-3430-1931

Francesco Di Renzo − *ICGM, CNRS, Université de Montpellier, ENSCM, Montpellier 34095, France*

Giulia Zambotti − *Istituto Nazionale di Ottica, INO-CNR, and Dipartimento di Ingegneria dell'Informazione, Università degli Studi di Brescia, Brescia 25121, Italy*

Marco Baù − *Istituto Nazionale di Ottica, INO-CNR, and Dipartimento di Ingegneria dell'Informazione, Università degli Studi di Brescia, Brescia 25121, Italy*

Marco Ferrari − *Istituto Nazionale di Ottica, INO-CNR, and Dipartimento di Ingegneria dell'Informazione, Università degli Studi di Brescia, Brescia 25121, Italy*

Vittorio Ferrari − *Istituto Nazionale di Ottica, INO-CNR, and Dipartimento di Ingegneria dell'Informazione, Università degli Studi di Brescia, Brescia 25121, Italy*

Complete contact information is available at: https://pubs.acs.org/10.1021/acsami.1c00625

Notes

The authors declare no competing financial interest.

ACKNOWLEDGMENTS

This work is part of the SCENT project, which has received funding from the ATTRACT project funded by the EC under Grand Agreement 777222. The ATTRACT consortium is not responsible for any use that may be made of the results. The synchrotron XRD experiments were performed at the Xpress beamline from Elettra Sincrotrone Trieste (proposal number: 20185087). The synchrotron IR experiments were performed at the SMIS beamline from Synchrotron SOLEIL (proposal number: 20181359). We acknowledge R. Borghes and V. Chenda for having improved the Xpress beamline software tools.

REFERENCES

(1) Drozdov, A. P.; Eremets, M. I.; Troyan, I. A.; Ksenofontov, V.; Shylin, S. I. Conventional Superconductivity at 203 Kelvin at High Pressures in the Sulfur Hydride System. *Nature* **2015**, *525*, 73−76.

(2) *High Pressure Process Technology: Fundamentals and Applications*; Bertucco, A., Vetter, G., Eds.; Elsevier Science B.V., 2001.

(3) Bundy, F. P.; Hall, H. T.; Strong, H. M.; Wentorfjun, R. H. Man-made Diamonds. *Nature* **1955**, *176*, 51−55.

(4) Wentorf, R. H. Cubic Form of Boron Nitride. *J. Chem. Phys.* **1957**, *26*, 956.

(5) Fitzgibbons, T. C.; Guthrie, M.; Xu, E.-s.; Crespi, V. H.; Davidowski, S. K.; Cody, G. D.; Alem, N.; Badding, J. V. Benzene-derived Carbon Nanothreads. *Nat. Mater.* **2015**, *14*, 43−47.

(6) Santoro, M.; Ciabini, L.; Bini, R.; Schettino, V. High-pressure Polymerization of Phenylacetylene and of the Benzene and Acetylene Moieties. *J. Raman Spectrosc.* **2003**, *34*, 557−566.

(7) Scelta, D.; Ceppatelli, M.; Santoro, M.; Bini, R.; Gorelli, F. A.; Perucchi, A.; Mezouar, M.; Van der Lee, A.; Haines, J. High Pressure Polymerization in a Confined Space: Conjugated Chain/Zeolite Nanocomposites. *Chem. Mater.* **2014**, *26*, 2249−2255.

(8) Santoro, M.; Scelta, D.; Dziubek, K.; Ceppatelli, M.; Gorelli, F. A.; Bini, R.; Garbarino, G.; Thibaud, J.-M.; Di Renzo, F.; Cambon, O.; Hermet, P.; Rouquette, J.; Van der Lee, A.; Haines, J. Synthesis of 1D Polymer/Zeolite Nanocomposites under High Pressure. *Chem. Mater.* **2016**, *28*, 4065−4071.

(9) Bässler, H. An Ideal 1D Quantum Wire? *Nat. Phys.* **2006**, *2*, 15−16.

(10) Kitao, T.; Uemura, T. Polymers in Metal-Organic Frameworks: From Nanostructured Chain Assemblies to New Functional Materials. *Chem. Lett.* **2020**, *49*, 624−632.

(11) Begum, S.; Hassan, Z.; Bräse, S.; Tsotsalas, M. Polymerization in MOF-Confined Nanospaces: Tailored Architectures, Functions, and Applications. *Langmuir* **2020**, *36*, 10657−10673.

(12) Wu, C.-G.; Bein, T. Conducting polyaniline filaments in a mesoporous channel host. *Science* **1994**, *264*, 1757−1759.

(13) Strandwitz, N. C.; Nonoguchi, Y.; Boettcher, S. W.; Stucky, G. D. In Situ Photopolymerization of Pyrrole in Mesoporous TiO_2. *Langmuir* **2010**, *26*, 5319−5322.

(14) Lee, W.-E.; Oh, C.-J.; Kang, I.-K.; Kwak, G. Diphenylacetylene Polymer Nanofiber Mats Fabricated by Freeze Drying: Preparation and Application for Explosive Sensors. *Macromol. Chem. Phys.* **2010**, *211*, 1900−1908.

(15) Dai, J.; Ogbeide, O.; Macadam, N.; Sun, Q.; Yu, W.; Li, Y.; Su, B.-L.; Hasan, T.; Huang, X.; Huang, W. Printed Gas Sensors. *Chem. Soc. Rev.* **2020**, *49*, 1756−1789.
(16) Polzonetti, G.; Russo, M. V.; Furlani, A.; Iucci, G. Interaction of H_2O, O_2 and CO_2 with the Surface of Polyphenylacetylene Films: an XPS Investigation. *Chem. Phys. Lett.* **1991**, *185*, 105−110.
(17) Baschenko, O. A.; Tyzykhov, M. A.; Nefedov, V. I.; Polzonetti, G.; Russo, M. V.; Furlani, A. Iodine Incorporation into Polymeric Films Investigated by Angle-Resolved XPS. *J. Electron Spectrosc. Relat. Phenom.* **1991**, *56*, 203−209.
(18) Alabarse, F. G.; Rouquette, J.; Coasne, B.; Haidoux, A.; Paulmann, C.; Cambon, O.; Haines, J. Mechanism of H_2O Insertion and Chemical Bond Formation in $AlPO_4$-54•xH_2O at High Pressure. *J. Am. Chem. Soc.* **2015**, *137*, 584−587.
(19) Alabarse, F. G.; Haines, J.; Cambon, O.; Levelut, C.; Bourgogne, D.; Haidoux, A.; Granier, D.; Coasne, B. Freezing of Water Confined at the Nanoscale. *Phys. Rev. Lett.* **2012**, *109*, 035701.
(20) Alabarse, F. G.; Brubach, J.-B.; Roy, P.; Haidoux, A.; Levelut, C.; Bantignies, J.-L.; Cambon, O.; Haines, J. $AlPO_4$-54 − $AlPO_4$-8 Structural Phase Transition and Amorphization under High Pressure. *J. Phys. Chem. C* **2015**, *119*, 7771−7779.
(21) Fabbiani, M.; Polisi, M.; Fraisse, B.; Arletti, R.; Santoro, M.; Alabarse, F.; Haines, J. An In-situ X-ray Diffraction and Infrared Spectroscopic Study of the Dehydration of $AlPO_4$-54. *Solid State Sci.* **2020**, *108*, 106378.
(22) Alabarse, F. G.; Silly, G.; Haidoux, A.; Levelut, C.; Bourgogne, D.; Flank, A.-M.; Lagarde, P.; Pereira, A. S.; Bantignies, J.-L.; Cambon, O.; Haines, J. Effect of H_2O on the Pressure-Induced Amorphization of $AlPO_4$-54•xH_2O. *J. Phys. Chem. C* **2014**, *118*, 3651−3663.
(23) Goldfarb, D.; Li, H. X.; Davis, M. E. Dynamics of Water Molecules in VPI-5 and A1PO4-5 Studied by ^2H NMR Spectroscopy. *J. Am. Chem. Soc.* **1992**, *114*, 3690−3697.
(24) Duer, M. J.; He, H.; Kolodziejski, W.; Klinowski, J. Dynamics of water in the Aluminophosphate Molecular-Sieve VPI-5 − a ^2H NMR-Study. *J. Phys. Chem.* **1994**, *98*, 1198−1204.
(25) Chauser, M. G.; Kol'tsova, L. S.; Vladimirov, L. V.; Urman, Y. G.; Alekseyeva, S. G.; Zaichenko, N. L.; Oleinik, E. F.; Cherkashin, M. I. An IR Spectroscopy and High Resolution ^1H NMR Study of Polyphenylacetylene Microstructures. *Polym. Sci.* **1988**, *30*, 1539−1546.
(26) Grey, C. P.; Veeman, W. S.; Vega, A. J. Rotational Echo $^{14}N/^{13}C/^1H$ Triple Resonance Solid-State Nuclear Magnetic Resonance: A Probe of ^{13}C-^{14}N Internuclear Distances. *J. Chem. Phys.* **1993**, *98*, 7711−7724.
(27) Schmidt-Rohr, K.; Spiess, H. W. *Multidimensional Solid-State NMR and Polymers*; Academic Press: London, 1994.
(28) Torad, N. L.; Lian, H.-Y.; Wu, K. C.-W.; Zakaria, M. B.; Suzuki, N.; Ishihara, S.; Ji, Q.; Matsuura, M.; Maekawa, K.; Ariga, K.; Kimura, T.; Yamauchi, Y. Novel Block Copolymer Templates for Tuning Mesopore Connectivity in Cage- Type Mesoporous Silica Films. *J. Mater. Chem.* **2012**, *22*, 20008−20016.
(29) Caliendo, C.; Verona, E.; D'Amico, A.; Furlani, A.; Iucci, G.; Russo, M. V. Surface Acoustic Wave Humidity Sensor. *Sens. Actuators, B* **1993**, *16*, 288−292.
(30) Venditti, I.; Bearzotti, A.; Macagnano, A.; Russo, M. V. Enhanced Sensitivity of Polyphenylacetylene and Poly-[Phenylacetylene-(Co-2-Hydroxyethyl Methacrylate)] Nanobeads to Humidity. *Sens. Lett.* **2007**, *5*, 1−5.
(31) Röck, F.; Barsan, N.; Weimar, U. Electronic Nose: Current Status and Future Trends. *Chem. Rev.* **2008**, *108*, 705−725.
(32) Bissell, R. A.; Persaud, K. C.; Travers, P. The Influence of Non-Specific Molecular Partitioning of Analytes on the Electrical Responses of Conducting Organic Polymer Gas Sensors. *Phys. Chem. Chem. Phys.* **2002**, *4*, 3482−3490.

https://doi.org/10.1021/acsami.1c00625
ACS Appl. Mater. Interfaces 2021, 13, 27237−27244